Article

Synthesis, Luminescence ,Absorption , Corrosion Properties and Study of Ionic Conductance in Solution for a (4-Hydroxy-3- Amino-1,8- Naphthalic Anhydride)

Khawla Sabeeh Burgal[1] and Roza Al-Aqar[1]

[1]Department of Chemistry, College of Science, Basrah University, Basrah, Iraq

https://orcid.org/0000-0001-9960-1313.

Email: rozachemistry@yahoo.co.uk.

Abstract

In this paper, the compound of (4-hydroxy-3-amino-1,8-naphthalic anhydride) and the dopant material (4-hydroxy-m-benzene-disulfonic acid) were synthesized. The UV- Vis absorption and fluorescence spectra of the compound were recorded, the compound 4- hydroxy-m- benzene-disulfonic acid was synthesized, the compound was characterized by the FT-IR spectroscopy. The absorption band is sensitive to the polarity of the solvent, for example in 1-butanol, showing only a slight red shift from 338 nm in 1-butanol to 340 nm in DMSO ($\Delta\lambda_{max}^{Abs}$ = 2 nm). The fluorescence spectra of this compound were sensitive to the polarity of the solvent, the compound showed a structured emission band displaying a slight red-shift from 375 nm in ethanol to 378 nm in DMSO, upon increasing the polarity of the solvent ($\Delta\lambda_{max}^{F}$ = 3 nm). The effect of the dopant material on the conductivities (ionic and specific) of the compound was studied, the ionic conductance was increased as the weight of the dopant material increases. The bathochromic shifts in absorption due to the polarity of the solvent were observed, for example, in ethanol, the compound had a λmax value at 338 nm and a red shift for the polar solvent at 340 nm, in DMSO solvent. The fluorescence was showed ca. 6 nm red shift on moving from 1-butanol to DMSO. Evaluation of the synthesized compound as corrosion inhibitors for carbon steel alloy C1010. (4-hydroxy -3- amino -1,8-naphthalic anhydride) as anti-corrosion agents for the C1010 alloy of carbon steel was studied.

Keywords: Bathochromic shifts, Conductance, Emission, Intramolecular hydrogen bonding, Solvent polarity.

1. Introduction

The naphthalimide derivatives are used because they are many good properties, for example excellent fluorophores with good quantum yield and high stability, and they are used in different applications, such as fluorescent chemosensors for metal anions and cations, and pH. The new optical chemosensors are prepared through potential carriers of these derivatives. The chemosensors are used in organic solutions because the groups of lipophilic alkyl or phenyl are connected to imide moieties of these derivatives[1,2]. Many 1,8-naphthalic anhydride derivatives are used as fluorescent dyes and fluorescent whitening agents[3,4]. The compound of 4-amino-phthalimide is displayed intramolecular charge transfer (ICT) fluorophore and is sensitive to the polarity of the solvent and also to intermolecular hydrogen bonding with a protic solvent, the fluorescence is quenched through the connection of hydrogen bonding between alcohol molecules and 4-aminophthalimides, the quenching is result from the promoted non-radiative methods by the intersystem crossing or/ and internal conversion. The non-radiative decay processes are depend on twisted intramolecular charge transfer (TICT) mechanism. The increasing of the quantum yields is obtained by the change of dialkyl amino group in 4-alkyl amino-1,8-naphthalimide with an aziridinyl group, and efficiency suppressed the process of deactivation by the TICT state. The compound of 6-dimethyl amino-2,3-naphthalimide (6-DMN) has been displayed the ICT fluorophore and showed positive solvatofluorochromism[5].

The labelling of nucleic acids or/ and oligonucleotides are detected through the fluorescent molecules, also these molecules are used for the covalent labelling of oligonucleotides, for example Rhodamine and pyrene. The different non-covalent and covalent interactions of oligonucleotides are investigated by many derivatives of naphthalic anhydride / naphthalimide, these derivatives which are fluorescent and used to study nucleic acids (i.e. chemical recognition) and photoinduced DNA[6]. The naphthalic imides are fluorescent molecules, and these compounds are interesting because many excellent chemical and physical properties, for example the stability (i.e. chemical and thermal) and the properties of the spectroscopy and electrochemistry and they are used as electron acceptors, which are allowed to use in the electron transfer processed. These compounds are solvatochromic and photoactive through photoinduced electron transfer and they used in optical sensors. Also, these compounds are used in the solid state, like n-type semiconductors, in order to design of electronic devices, such as transistors

and OLEDs also[7]. The 4-amino-1,8-naphthalimide has been used as the fluorophore moiety, and the chemical probes has been designed through the naphthalimide compound, because the naphthalimide derivatives are showed many excellent properties, which have a strong absorption in the visible region and large Stokes shift[8]. 4-amino-1,8-naphthalimide can be used in the living cells as a fluorescent sensor, and the compound has fluorescence improved based on the process of photoinduced electron transfer (PET), this process which occurs between the interaction of photoactive materials and the light. The fluorophore-spacer-receptor (ionophore) is used to design a PET-type fluoroionophore[9]. Different synthetic organic compounds containing a suitable receptor, for example 4-amino-1,8-naphthalimide derivatives have been used for the studies of sensitive ion-receptor interaction[10]. The 4-amino-1,8-naphthalimides has showed the internal charge-transfer (ICT) excited states, with side-chains of aminoalkyl and revealed unidirectional PET processes. The 4-amino group appears a PET process when the former is connected to this group of the fluorophore[11].

Corrosion and pollution are two major difficulties that have an impact on earth's living beings among many other grave challenges that influence human life. The first issue is determined by the fundamental thermodynamic action or process along with a reduction in Gibb's free energy[12]. The effects of corrosion on industrial applications and processes are well documented, particularly when it comes to expensive protective techniques or maintenance of metallic or non-metallic materials[13]. The degradation or destruction of materials as a result of a material's interaction with its environment is known as corrosion. Organic or inorganic substances can prevent corrosion. Adsorbed layer formers called organic inhibitors strongly adsorb to metal surfaces and interfere with cathodic and anodic reactions in the vicinity of the adsorption. In this study, chemicals' ability to successfully inhibit a particular system is frequently influenced by the chemical structure of the inhibitor molecule[14,15].

In the current work, we report on the preparation of 4-hydroxy-3-amino-1,8-naphthalic anhydride. The UV- visible absorption and emission spectral properties and ionic conductance were studied. Application in conductance by using dopant material (4-hydroxy-m-benzene-disulfonic acid) was investigated.

2. Materials and Methods

2.1. Synthesis of 4-hydroxy-3-amino-1,8-naphthalic anhydride

4-hydroxy-3-nitro,1,8-naphthalic anhydride, (15 gm, 0.058 mole), tin (II) chloride (50 gm, 0.26 mole) and concentrated hydrochloric acid (80 ml) was

stirred for 2h at (80-85)^{O} C, the mixture was cooled and filtered, then washed with 5% HCl and water then dried [16]., (Scheme 1).

2.2. Synthesis of of 4- hydroxy-m- benzene-disulfonic acid

In a dry 500 ml (flat – bottomed flask), was placed 31 gm (0.33 M) of phenol and then mixed with 116 gm of concentrated sulphuric acid. The mixture was heated in a boiling water bath with 3 hr with mechanical stirrer. The mixture was cooled to room temperature or below by immersing the flask in ice water, and a solution of (95 gm of NaOH in 235 mL water) was added slowly, the solid salt was separated[17].

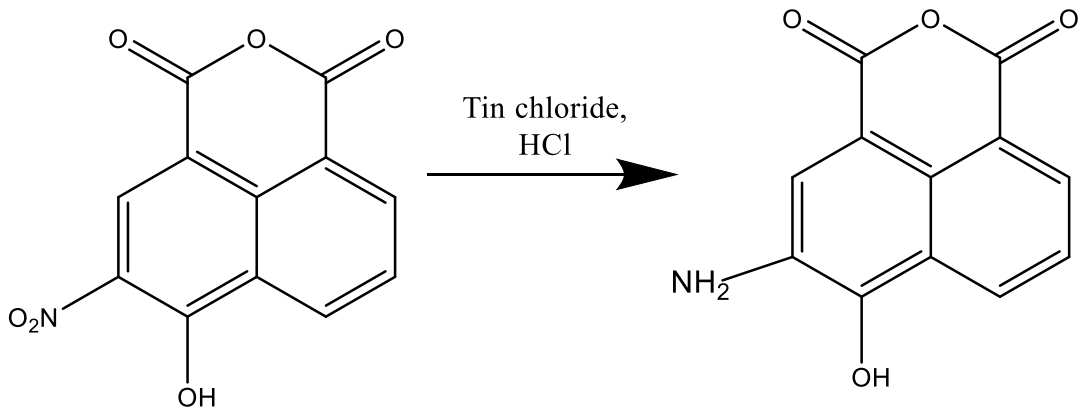

Scheme 1. The synthesis of 4-hydroxy-3-amino-1,8-naphthalic anhydride.

2.3. Evaluation of the synthesized compound as corrosion inhibitors for carbon steel alloy C1010

The synthesized chemical in this study was evaluated using the Tafel plot method. 1,8-naphthalic anhydride (4-hydroxy -3- amino -1,8-naphthalic anhydride) as anti-corrosion agents for the C1010 alloy of carbon steel were studied.

2.4. The Electrochemical Cells

Image depicts the electrochemical test cell utilized in this investigation in (Fig. 1). Three electrodes are connected to a (1000 mL) vessel make up the cell, which was set up as follows, a functioning electrode (carbon steel specimen), electrode of reference (Silver in AgCl solution), opposing electrode (Platinum).

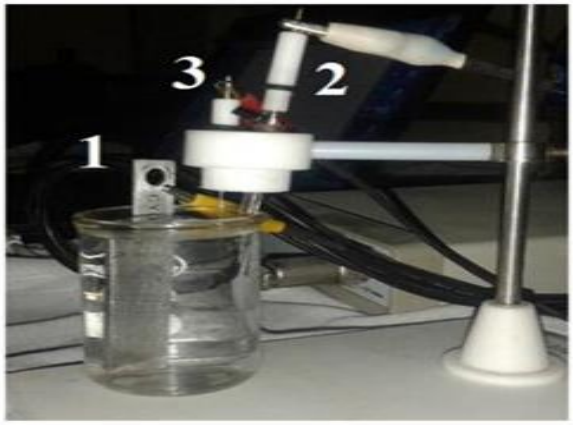

Figure 1. The measurements of corrosion's electrochemical cell.

2.5. Experimental Procedure for Tafel Plot Method

Setting up the Tafel experiment, to determine the corrosion rates, a potentiostat was utilized to measure electric potential vs. current density. The device utilizes a variety of methods, including Tafel plots. Alternative measurement methods, such as potentiodynamic polarization scan and linear polarization scan are used.

2.6. The Composition of Alloys

We employed one sort of carbon steel alloy in this study(C1010) with (3) cm in length, (1.24) cm in width, and (0.14) cm in thickness. The alloy is made up of standard strips that were purchased from the Alabama company Metal Samples U.S.A., and its composition is shown in (Table 1) .The total area of immersed strip is 8.45cm^2. The chemical make-up of the carbon steel alloy C1010 is shown in (Table 1).

Table 1. The chemical make-up of the carbon steel alloy C1010.

Alloy, Carbon steel (C1010)	C	S	P	Mn	Ni	Si	Cr	Cu	As	Fe
Composition % w/w	0.13	0.05	0.04	0.30	0.30	0.37	0.10	0.30	0.08	Balance

Preparing the carbon steel samples[18].

1. Differentiated smoothness Silicon carbide paper was used to carry out the grinding procedure (100,120,200,400,600,1000,1200).

2. Using distilled water and ethanol to wash the specimens to remove any remaining dirt and rust on the iron.

3. The sample was moved to the polishing system, where it was placed on the turntable and covered with a soft cloth. movement , the disc's rotation was reversed, alumina was added, and it was polished to remove any scratches.

4. Following polishing, the sample was cleaned with distilled water before spending around 15 minutes submerged in acetone.

5. To keep the samples safe from moisture, they were kept in desiccators that contained silica gel.

2.7. Solution preparations

Each synthetic inhibitor was made separately at doses of 2, 4, and 6 ppm at various temperatures of 298, 308, and 328 k in a corrosive environment of (0.1) N of HCl (blank). By using the corrosion instrument, the corrosion measurements were acquired.

3. Results and discussion

3.1. The photophysical properties (UV- Visible absorption)

The UV- Visible absorption of the compound 4- hydroxy-3-amino-1,8-naphthalic anhydride in different solvents, for example dimethyl sulfoxide DMSO, ethanol, and 1-butanol was recorded to study its spectral properties in many solvents of different polarity (Fig. 2,3,4). The wavelengths corresponding to the spectral peaks are shown in (Table 2).

Table 2. Absorption and emission data for the compound (4- hydroxy-3-amino-1,8- naphthalic anhydride) in different solvents.

Solvents	Absorption maxima (nm)	Fluorescence maxima (nm)
ethanol	240, 338	375
1-butanol	240, 338	372
DMSO	340	378, 302

The compound showed a structured absorption bands in the 240 nm and 338 nm in ethanol solvent indicate that the character of the band is of an allowed π, π* transition 338 nm. The absorption band is sensitive to the polarity of the solvent, for example in 1-butanol, showing only a slight red shift from 338 nm in 1-butanol to 340 nm in DMSO ($\Delta\lambda_{max}^{Abs}$ = 2 nm). The absorption was sensitive to the solvent polarity due to intramolecular hydrogen bonding and the conjugation between the amino group and the imide group in the ground state for the naphthalimides compounds[5]. The compound has structured absorption (there appear to be two peaks) in ethanol and 1-butanol solvents, which could be attributed to the lowest π, π* transitions. On the other hand, bathochromic shifts in absorption due to the

polarity of the solvent were observed. For example, in ethanol, the compound had a λ_{max} value at 338 nm and a red shift in absorption for the polar solvent DMSO at 340 nm. It is interesting to observe the effect of the substituents at C-4 on the spectrum of the absorption, such as some groups had strong electron-donating , for example alkoxy and alkyl amine[19]. The compound shows one absorption peak at 338 nm, which may be assigned to the intramolecular charge transfer (ICT) band, and the second band at 240 nm in the UV region, which could be assigned to the $\pi \rightarrow \pi^*$ transition of the naphthalic ring[20]. In DMSO solvent, the absorption maximum is 2 nm bathochromically shifted than that in ethanol solvent, this could be attributed to the electron donating amino group, therefore the strength of the intramolecular hydrogen is increased[21].

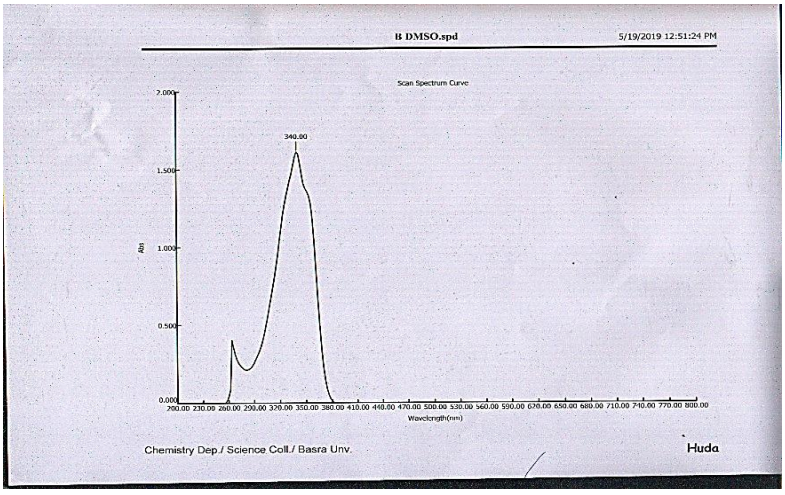

Figure 2. The UV- Visible in DMSO solvent.

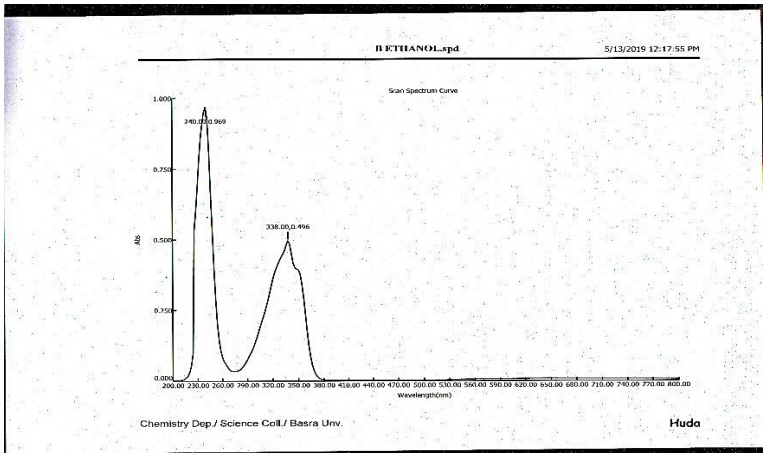

Figure 3. The UV- Visible in ethanol solvent.

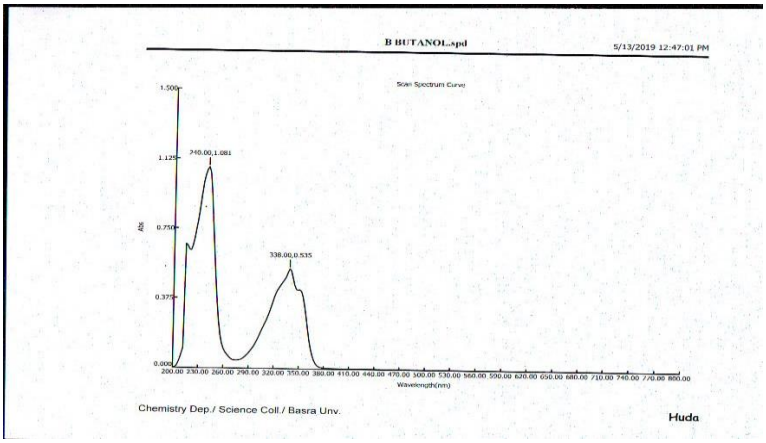

Figure 4. The UV- Visible in 1-butanol solvent.

3.2. The fluorescence spectra

The fluorescence spectra of the compound (4-hydroxy-3-amino-1,8-naphthalic anhydride) are shown in (Fig. 5,6,7). It can be showed from the Figures, that the fluorescence spectra of this compound were sensitive to the polarity of the solvent (Table 2). The compound showed a structured emission band displaying a slight red-shift from 375 nm in ethanol to 378 nm in DMSO, upon increasing the polarity of the solvent ($\Delta\lambda^{F}_{max}$ = 3 nm). It can be seen that intramolecular hydrogen bonding between amino hydrogen and carbonyl oxygen that was described over the intermolecular hydrogen bonding with alcohol[5]. The emission band of the compound also blue-shifted from 375 nm in ethanol to 372 nm in 1-butanol, displaying a solvent from ethanol to 1-butanol. The small red shift on the maximum emission band of this compound in polar solvents compared with in less polar solvents can be seen from the spectra, this is because the polar solvents are stabilized to the polar ICT excited states and therefore the energy gap between the ground and excited states is decreased and leads to small red shift on the maximum emission peak[20]. The fluorescence properties were found effect on the solvent (medium) polarity, showing *ca*. 6 nm red shift on moving from 1-butanol to DMSO. In general, the related 4-amino-1,8-naphthalimides have ICT character in the excited states[22]. The solvent polarity is caused a red shift between the polar and nonpolar solvents; therefore the fluorescence intensity was shifted to a longer wavelength as the polarity of the solvent was increased[23]. The excited state of the lowest singlet is almost $\pi \rightarrow \pi^*$ in nature, which is responsible for the fluorescence, and the stabilization is agreement with a $n \rightarrow \pi^*$ nature of the emitting state, by the decreasing of the solvent polarity[24].

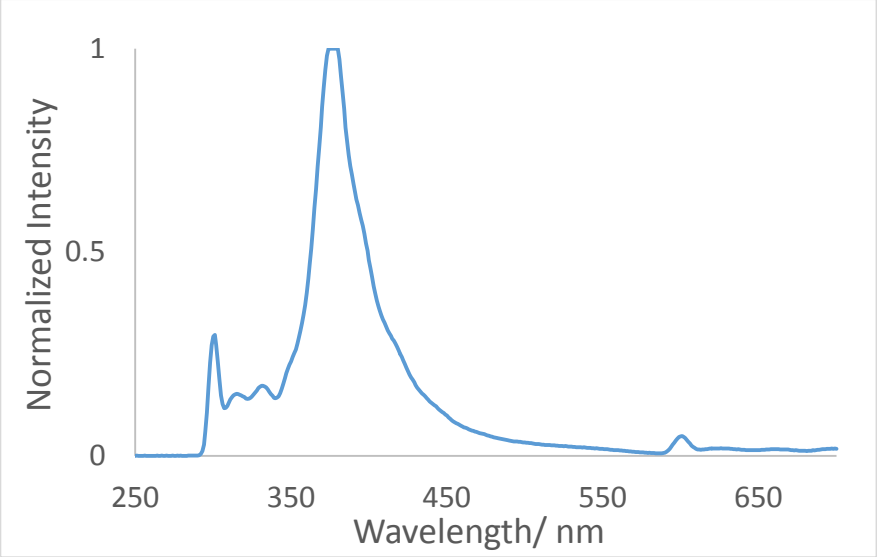

Figure 5. The fluorescence spectrum in DMSO.

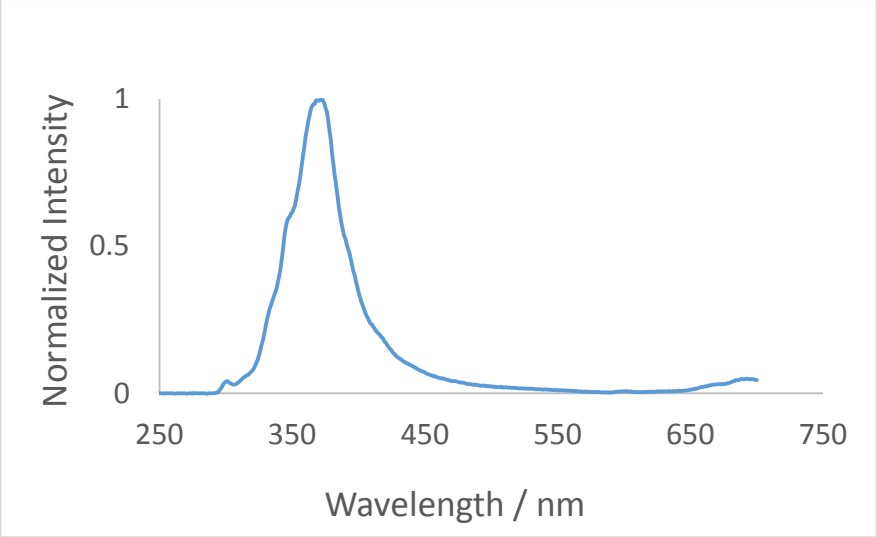

Figure 6. The fluorescence spectrum in 1-butanol.

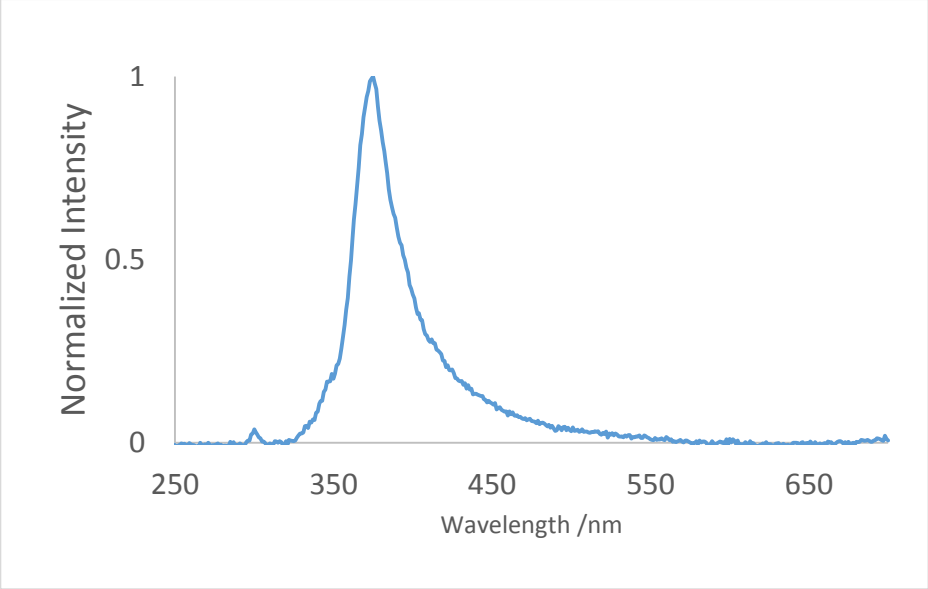

Figure 7. The fluorescence spectrum in ethanol.

3.3. FT-IR spectroscopy

The FT-IR was used for the characterization of the compound (4-hydroxy-3-amino-1,8-naphthalic anhydride), the FT-IR data showed stretching band at 1570 cm^{-1} for C=C, and the band at 3066 cm^{-1} for the C-H stretching, and the band at 3444 cm^{-1} for the N-H primary amine. The bands at 1735, 1778 cm^{-1} for C=O stretching[25]. The C-N band at 1134 cm^{-1}, and OH band at 3444 cm^{-1} and C-O-H at 1022 cm^{-1} [26], the aromatic C-H bending at about 1022 cm^{-1} [24].

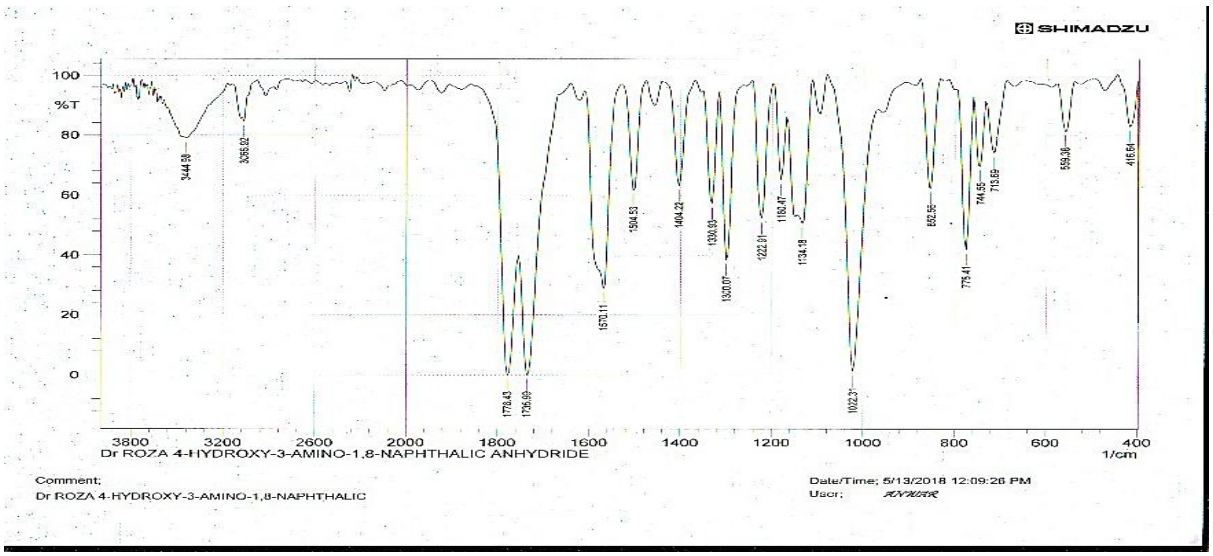

Figure 8. The FT-IR spectrum for the compound.

3.4. Corrosion inhibition

(4-Hydroxy-3- amino -1,8-naphthalic anhydride) as corrosion inhibitors

Because of the metal deterioration brought on by chemical or electrochemical processes, metals or alloys like carbon steel corrode, on the outside of carbon steel. Inhibitors can be added to lessen or control it, such is organic substances that result in the carbon steel's surface being protected from corrosion. Corrosion inhibitors for C10C10 carbon steel alloy were utilized in this investigation. For carbon steel, alloy C10C10 in the absence and presence of a specific inhibitor in relation to corrosive hydrochloric acid medium (0.1 N), electrochemical data obtained by employing Tafel plots is provided in the (Table 3)

Moreover, these tables present additional electrochemical data derived from the polarization curves, including corrosion current density Icorr, Tafel constants (βa and βc), polarization resistance (Rp), inhibitions efficiency (IE%), corrosion potential (ECorr), and surface coverage area (Ɵ) Increasing the concentration of the aforementioned inhibitors has a considerable impact on and affects all of those parameters.

$$CR_{mpy} = \frac{0.13xIcorrxEq.wt.}{AxD} \quad (1)$$

Eq.Wt. stands for the equivalent weight of corroding species (g/eq), D for the corroding species' density (g/cm^3), and CR stands for corrosion rate as measured by (mpy), A is the corrosion current density (mA/cm^2) and Icorr is the area of the corroding species (cm^2). The Analysing of the corrosion inhibitors by using the equation 2.

$$IE\% = \frac{CR° - CR}{CR°} x100 \quad (2)$$

Corrosion rate of the uninhibited system is CR$^\circ$, while IE stands for inhibitor effectiveness. CR stands for the inhibited system's corrosion rate. The following formulae can be used to compute the surface area of the metal that the inhibitor coated on the surface of the metal or alloy.

$$\theta = \frac{CR° - CR}{CR°} \quad (3)$$

The charge transfer resistance of the metal or alloy in the presence of acid media and the absence of an inhibitor is represented by the surface coverage area, respectively.

Table 3. 4-Hydroxy-3- amino -1,8-naphthalic anhydride as Corrosion Inhibitor at (2-6) ppm against corrosive medium of 1N of HCl at (298-323)k.

Comp	Conc. ppm	Temp(K)	CR	Rp (ohm)	$I_{\circ}$ (µA)	$E_{\circ}$ (mV)	βC (mV/de)	βa (mV/de)	θ	%IE
HCl	3650	298	317.23	337.12	685.06	-474	-8233	164.7		
2			38.4	1488.5	16.78	-768	-611	276	0.8734	87.34
4			33.5	518.6	41.08	-725	-606	272.3	0.8931	89.31
6			26.36	352.79	51.45	-686	-541.32	643.42	0.917	91.7
HCl	3650	308	525.4	941	1914.4	-680	-1863.7	179.45		
2			23.36	360.45	50.37	-678	-444.2	474.3	0.9258	92.58
4			16.34	509.67	36.32	-682	-366.7	436.49	0.9477	94.77
6			13.65	610.64	29.48	-681	-356.89	424.04	0.9563	95.63
HCl (50)		323	885.45	941	1912.3	-678	-1165.4	193.53		
2			71.23	308.64	583.2	-704	-392.4	397.51	0.9142	91.42
4			53.23	236.1	762.5	-675	-377.9	271.4	0.938	93.8
6			28.59	291.49	61.75	-517	-329.14	71.34	0.966	96.6

In this investigation, different doses of hydrochloric acid were used to test the produced compound's effectiveness as corrosion inhibitors. Then, at various temperatures, the impact of temperature on the inhibitor for a minimum and ideal concentration was investigated, by employing Tafel plot techniques at (25°C, 35°C, and 55°C). To assess the effectiveness of a corrosion inhibitor for carbon steel (C1010) alloy, 0.1N HCl solution was used in corrosive media at (25°C) (298) k, and different concentrations (2, 4 and 6) ppm was used to calculate the corrosion rate of the specified alloy in both the presence and absence of the specific inhibitor in order to assess the effectiveness of the inhibitor. The electrochemical data was given by the Tafel method, including the corrosion rate (CR) in mpy, the corrosion current density (Icorr) in $A.cm^2$, the charge transfer resistance (Rct) in, etc. Anodic and cathodic Tafel constants (βa and βc) and corrosion potential (ECorr) in mV, decade is used to refer to the current decade[27]. At three temperatures (298 and 323 k), the influence of temperature on the alloy corrosion rate and the inhibitor efficiency were each individually evaluated[28].

The change of 4-hydroxy-3- amino-1,8-naphthalic anhydride at various temperatures is given in (Fig. 9).

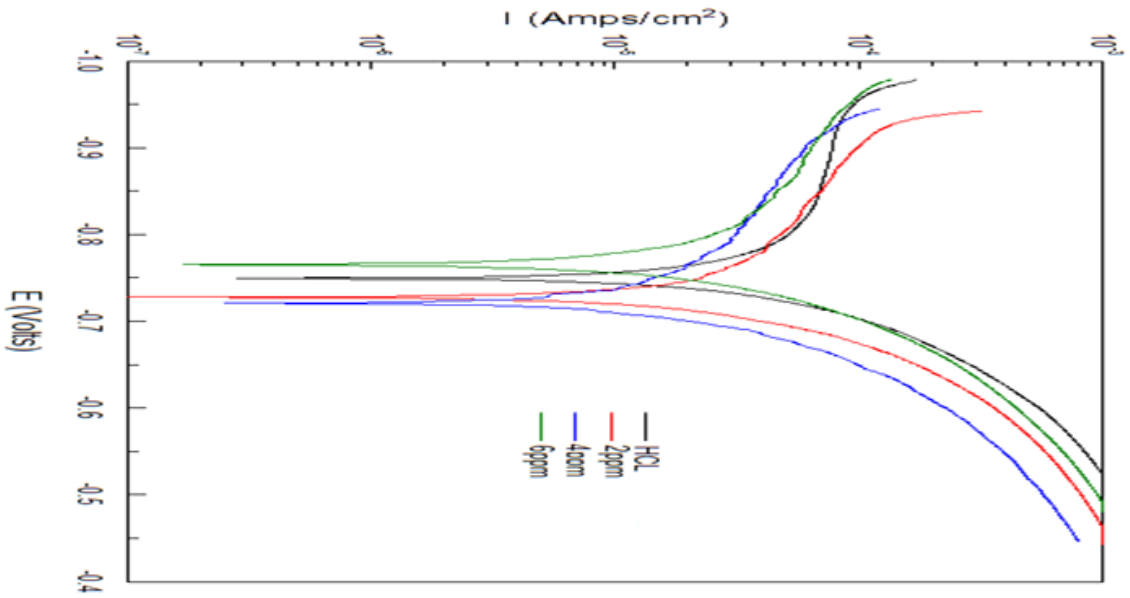

Figure 9. Tafel plot for carbon steel at 298 K in the presence and absence of 4-hydroxy-3- amino-1,8-naphthalic anhydride at various concentrations.

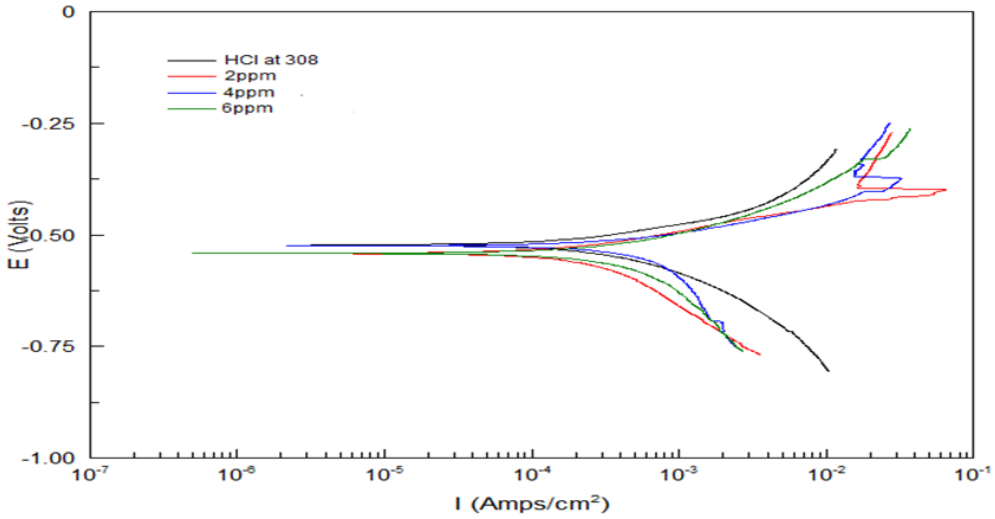

Figure 10. Tafel plot for carbon steel at 308 K in the presence and absence of 4-hydroxy-3- amino-1,8-naphthalic anhydride at various concentrations.

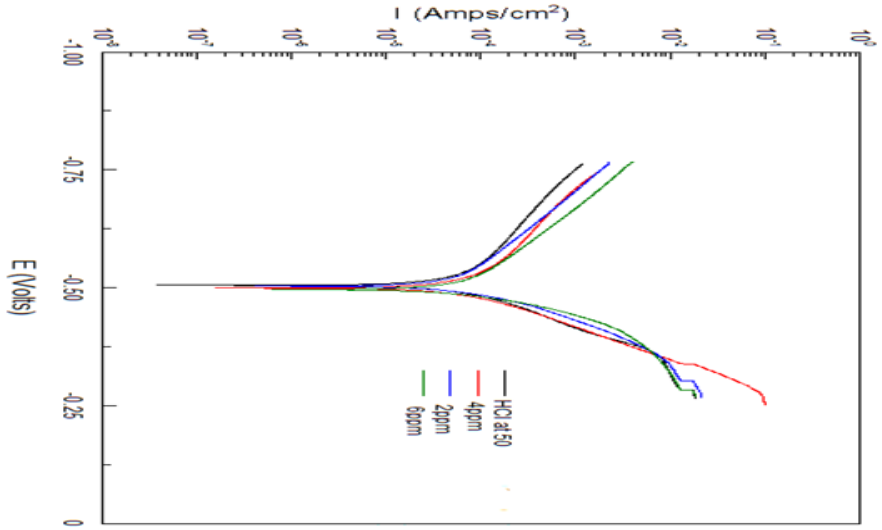

Figure 11. Tafel plot for carbon steel at 323 K in the presence and absence of 4-hydroxy-3- amino-1,8-naphthalic anhydride at various concentrations.

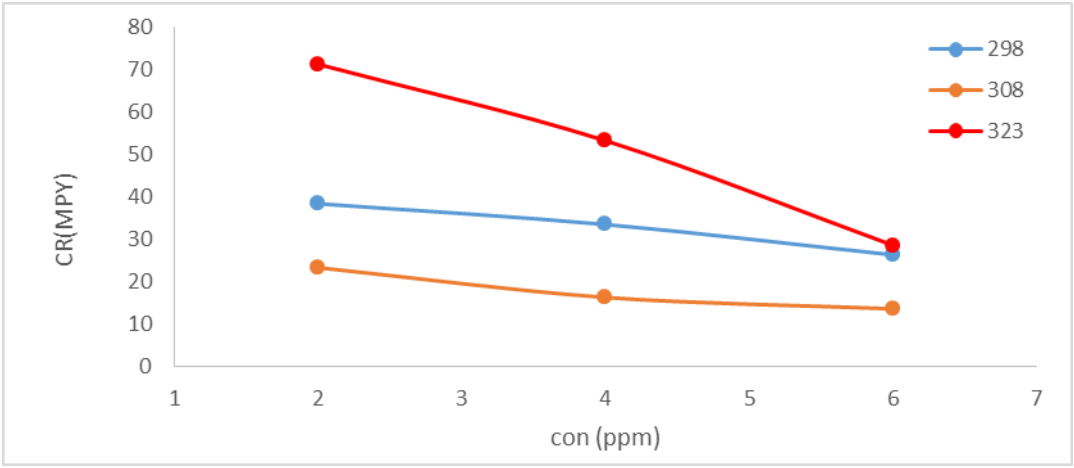

Figure 12. The relationship between the inhibitor concentration at various temperatures and the corrosion rate of carbon steel alloy in HCl (0.1N).

On the other hand, it was calculated the activation of energy Ea*, enthalpy of activation H*, entropy of activation S*, and Gibbs free energy of activation for the C1025 alloy. The kinetic of corrosion reaction on the carbon steel alloy in the presence and the absence Inhibitors was studied. The influence of temperature on a certain alloy's corrosion rate in the presence and absence of each artificial inhibitor for the least .The calculation of kinetic characteristics, such as the activation of the energy, was used to compare the concentration (2 ppm) and the calculation of kinetic parameters like the activation of the energy allowed for the study of the ideal concentration (6 ppm), with the ideal concentration (6) ppm, (Ea), activation enthalpy (H*), activation entropy (S*), and activation Gibbs free energy (ΔG*) .

The Arrhenius equation, equation 4 was used to calculate the activation energy value for the research of the impact of temperature.

$$lnCR = ln\, A - Ea/RT \quad (4)$$

Where: CR is corrosion rate (mpy), Ea is activation energy (KJ/ mol), A is frequency factor, R is molar of the gas constant (8.3143 $J.K^{-1}.mol^{-1}$), T is the temperature (k), the calculation of the activation of energy for the corrosion process of the aforementioned alloy in the presence and absence of the synthetic inhibitors was shown in Figure 13[29,30].

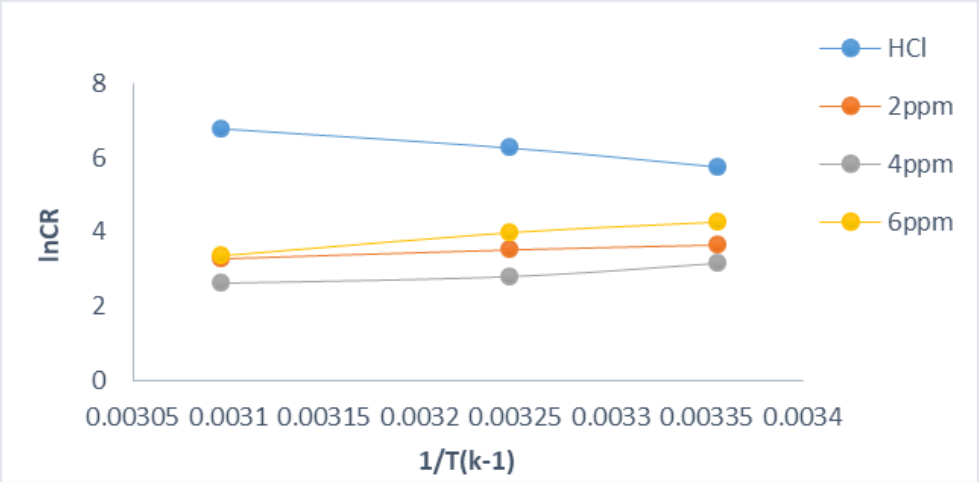

Figure 13. The Arrhenius relationship for the carbon steel alloy's corrosion reaction in the absence of an inhibitor.

On the other hand, the following equation, equation 5 is used to compute ΔS* and ΔH* for the corrosion reaction in the presence and absence of the inhibitor.

$$Ln\ CR/T = ln\ R/Nh + (\Delta S^*)/(R\ ) - (\Delta H^*)/RT \quad (5)$$

By plotting ln(CR/T)) against (1/T) to get a straight line, the slope is (ΔH*)/RT) while intercept is $ln(\ R/Nh + (\Delta S^*)/(R\ ))$ where, N is Avogadro's number 6.023 $x10^{23}$ $mole^{-1}$ and h is Plank's constant $6.625x10^{-34}$ J.S[31]. Moreover, the Gibbs-Helmholtz equation, equation 6 is used to calculate Gibbs free energy of activation.

$$\Delta G^* = \Delta H^* - T\Delta S^* \quad (6)$$

As a result, the activation data that was collected was summarized in the (Table 4) below:

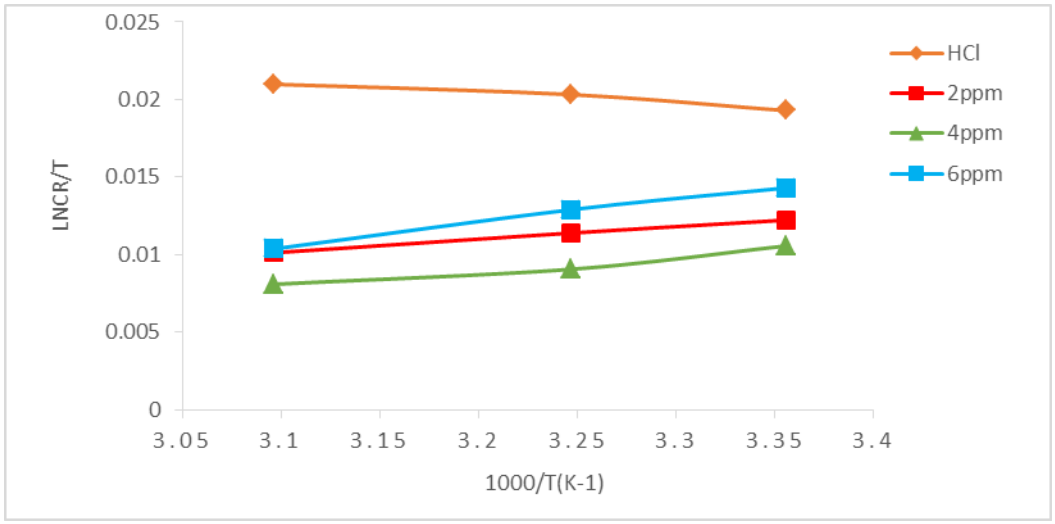

Figure 14. is shown Computation of the H* and S* for the Corrosion Reaction of the Carbon Steel Alloy in the Presence and Absence of the Inhibitor.

Table 4. Thermodynamic activation functions for the corrosion response of carbon steel alloy in the presence and absence of inhibitors.

Constituents	Con. ppm	Ea* ($_{KJ.mol}^{-1}$)	ΔH* ($_{KJ.mol}^{-1}$)	ΔS ($_{(JK\ mole}^{-1\ -1}$)	ΔG*($_{KJ.mol}^{-1}$)			A(s)
					298	308	323	
HCl (0.1N)	3650 (ppm)	32.705.96	53.2	-75.272	75.64	76.39	70.67	$17.4x10^{8}$
4-hydroxy-3-amino-1,8-naphthalic anhydride	2	-12.1156	-68.17	-75.682	-45.62	-44.86	-50.61	$29.1x10^{-5}$
	4	-16.7492	-78.15	-75.725	-55.58	-54.82	-60.58	$25x10^{-5}$
	6	-29.5341	-126.3	75.841	-103.77	-103.01	-108.77	$49.1x10^{-4}$

(Table 4) The graph above shows that the Arrhenius pre-exponential factor is higher when the inhibitors under study are present than when they are not. This is caused by an increase in the corrosion species' migration toward the inhibitor molecules, forming a stable adsorbed coating on the alloy's surface. This is consistent with the activation energy figures for the of the alloy in the presence of any one of the aforementioned inhibitors is greater than in absence, indicating that the inhibitor reduces the corrosion reaction[31-33]. The corrosion reaction, on the other hand, exhibits exothermic activity, or is triggered by a rise in temperature, as indicated by the standard enthalpy of activation, which is negative. In addition, whether the inhibitor is present or not, the entropy of activation is negative[34]. demonstrates that the presence of the inhibitor increases the tendency of the

corrosion reaction to create a stable activated complex as a rate-determining step[35]. According to the Gibbs free energy of activation, the spontaneous corrosion process accelerated in the presence of corrosion at all temperatures. It rose as temperature climbed, insisting that the adsorption of certain inhibitors increased as temperature increased, from 298K to 323K. It was established that the behaviour of chemical adsorption is revealed by a rise in inhibition efficiency with temperature, as well as when the Gibbs free energy value is more than 50 $kJ.mol^{-1}$ [36, 37].

3.5. The measurement of the ionic conductance

The ionic conductance G was measured in water, as a solvent. The influence of the dopant material 4- hydroxy-m- benzene-disulfonic acid on the conductivities of this compound is shown in (Fig. 15,16). It is shown that the conductance increases as the dopant material weights increases, (Table 5) , the G of the compound was $2.5x10^{-5}$ Siemens at 0.01 gm of the dopant material, while the value was $2.57x10^{-4}$ Siemens at 0.1 gm of the dopant material, (Fig. 16) shows the relationship between the weights of the dopant material and the specific conductance κ, the same behaviour was observed in the ionic conductance.

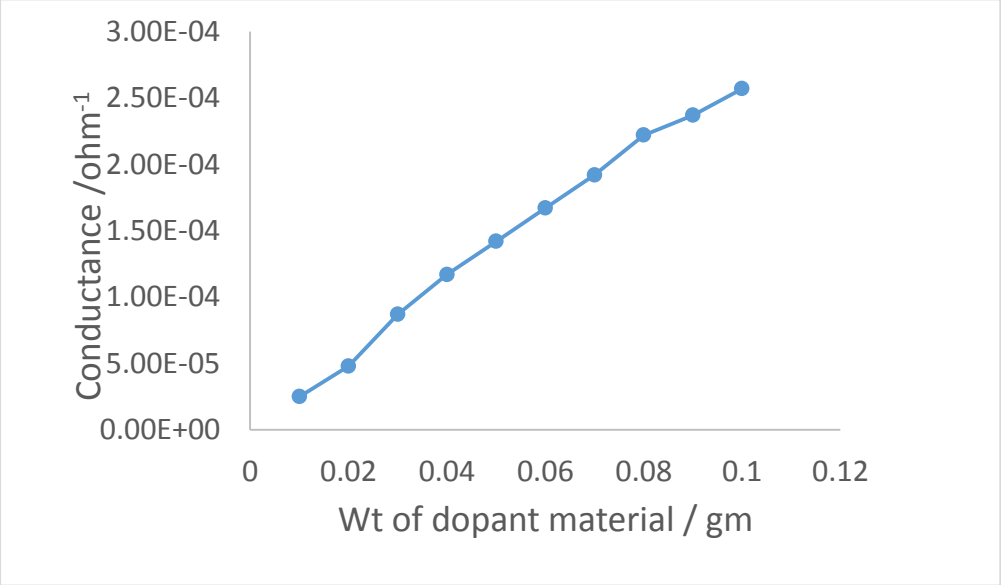

Figure 15. The conductance for the compound.

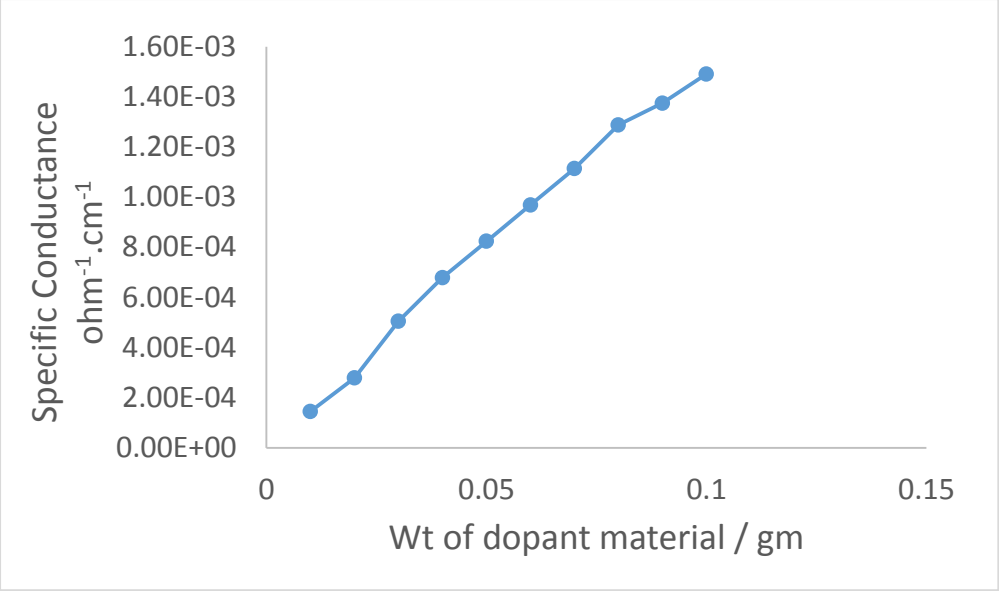

Figure 16. The specific conductance for the compound.

Table 5. The values of conductance and specific conductance for the compound after doped with the dopant material.

Weight /gm	Conductance /ohm^{-1}	Specific Conductance/ ohm^{-1}.cm^{-1}
0.01	2.50E-05	1.45E-04
0.02	4.80E-05	2.78E-04
0.03	8.70E-05	5.05E-04
0.04	1.17E-04	6.79E-04
0.05	1.42E-04	8.24E-04
0.06	1.67E-04	9.69E-04
0.07	1.92E-04	1.11E-03
0.08	2.22E-04	1.29E-03
0.09	2.37E-04	1.37E-03
0.1	2.57E-04	1.49E-03

4. Conclusion

The compound of (4-hydroxy-3-amino-1,8-naphthalic anhydride) and the dopant material (4-hydroxy-m-benzene-disulfonic acid) were synthesized, the bathochromic shifts in absorption due to the polarity of the solvent were observed. For example, in ethanol, the compound had a λ_{max} value at 338 nm and a red shift in absorption for the polar solvent DMSO at 340 nm, in DMSO solvent, the

absorption maximum is 2 nm bathochromically shifted than that in ethanol solvent, this could be attributed to the electron donating amino group, therefore the strength of the intramolecular hydrogen is increased. The fluorescence properties were found effect on the solvent (medium) polarity, showing *ca*. 6 nm red shift on moving from 1-butanol to DMSO. In general the related 4-amino-1,8-naphthalimides have ICT character in the excited states. The solvent polarity is caused a red shift between the polar and nonpolar solvents, therefore the fluorescence intensity was shifted to a longer wavelength as the polarity of the solvent was increased.

Acknowledgment

This research was undertaken with the assistance of College of Science at the University of Basrah, Chemistry department.

References

[1] LI, Chun-Yan, Zhou Y, Xu F, Li YF, Zou CX, Weng C. A fluorescent pH chemosensor based on functionalized naphthalimide in aqueous solution. AnalyticalSciences.2012;28(8):743-747.https://doi.org/10.2116/analsci.28.743.

[2] Wei Z, Yalei M, Hongwei S , Rong M, Jie K , Meng Z. Deciphering the photophysical properties of naphthalimide derivatives using ultrafast spectroscopy. Phys. Chem. Chem. Phys. 2024; 26: 4607-4613. https://doi.org/10.1039/d3cp05654f.

[3] Xuhong Q, Zhenghua Z, Kongchang C. The synthesis, application and prediction of stokes shift in fluorescent dyes derived from 1, 8-naphthalic anhydride. Dyes and Pigments. 1989; 11(1): 13-20. https://doi.org/10.1016/0143-7208(89)85022-3.

[4] Radu IT, Anton A, Florentina G, Alina N, Calin D. Photophysical Properties of Some Naphthalimide Derivatives. Eng. Proc. 2022; 27(1),4. https://doi.org/10.3390/ecsa-9-13356.

[5] Wang L, Fujii M, Yamaji M, Okamoto, H. Fluorescence behaviour of 2-, 3- and 4-amino-1, 8-naphthalimides: effects of the substitution positions of the amino functionality on the photophysical properties. Photochem. Photobiol. Sci. 2018; 17(10): 1319-1328. https://doi.org/10.1039/c8pp00302e.

[6] Singh Y, Misra A, Misra K. Syntheses, characterisation and fluorescence study of some novel naphthalimide derivatives. Indian J. Chem. 2002;41B: 1238-1245. http://hdl.handle.net/123456789/21934.

[7] Konstantinova T, Spirieva A, Petkova T. The synthesis, properties and application of some 1,8-naphthalimide dyes. Dyes Pigm. 2000; 45(2): 125-129. https://doi.org/10.1016/S0143-7208(00)00014-0.

[8] Shen K, Mao S, Shi X, Aderinto SO, Xu Y, Wu, H. Development of a New 4-Amino-1,8-Naphthalimide Derivative as a Fluorescent Probe for Monitoring the Divalent Copper Ion. J. Appl. Spectrosc. 2018;85:665-672. https://doi.org/10.1007/s10812-018-0702-9.

[9] Liu DY, Qi J, Liu XY, He HR, Chen JT, Yang GM. 4-Amino-1,8-naphthalimide-based fluorescent sensor with high selectivity and sensitivity for Zn2+ imaging in living cells. Inorg. Chem. Commun. 2014; 43: 173-178. https://doi.org/10.1016/j.inoche.2014.02.035.

[10] Misra A, Shahid M, Dwivedi P, Srivastava P, Ali R, Razi SS. A simple naphthalimide-based receptor for selective recognition of fluoride anion. ARKIVOC. ii. 2013: 133- 145. http://dx.doi.org/10.3998/ark.5550190.0014.212.

[11] De Silva AP, Goligher A, Gunaratne HN, Rice, TE. The pH-dependent fluorescence of pyridylmethyl-4-amino-1,8-naphthalimides. ARKIVOC. Vii. 2003: 229- 243. http://dx.doi.org/10.3998/ark.5550190.0004.720.

[12] Mohammed MT. Development of a new metastable beta titanium alloy for biomedical applications, KIJOMS. 2017; 3(4): 224-230. https://doi.org/10.1016/j.kijoms.2017.08.005.

[13] Haleem AH. Active inhibitor as corrosion protective of carbon steel. JUK. 2008; 6(1):196-207. a43da858e3ea0c0d.

[14] Matlob LDFK, Amir AMA, Hassan NF. Effect of using corrosion inhibitors on concrete properties and their activity. JUK. 2008; 6(4): 121-139. 15aa4448b7e08394.

[15] Ali FH, Al-Shimiesawi T, Hammud KK, Rahmman SA. Carbon steel corrosion inhibition in acidic medium by expired drugs. The Fifth Scientific Conference of the College of Science University of Kerbala journal of kerbala university. 2017; 11 (3): 115-126. be84eec3abd92fd0.

[16] Tan S, Yin H, Chen Z, Qian X, Xu Y. (2013). Oxo-heterocyclic fused naphthalimides as antitumor agents: Synthesis and biological evaluation . Eur. J. Med. Chem. 2013; 62 : 130-138. https://doi.org/10.1016/j.ejmech.2012.12.039.

[17] Kahol PK, Kumar KS, Geetha S, Trivedi DC. Effect of dopants on electron localization length in polyaniline. Synth. Met. 2003; 139(2) : 191-200. https://doi.org/10.1016/S0379-6779(02)01321-8.

[18] Li G, Szostak M. Kinetically controlled, highly chemoselective acylation of functionalized grignard reagents with amides by N− C cleavage. Chemistry–A European Journal. 2020;26(3):611-615. https://doi.org/10.1002/chem.201904678.

[19] Xiao H, Chen M, Shi G, Wang L, Yin H, Mei C. A novel fluorescent molecule based on 1,8-naphthalimide: synthesis, spectral properties, and application in cell imaging. Res Chem Intermed. 2010; 36 :1021- 1026. https://doi.org/10.1007/s11164-010-0214-6.

[20] Wang L, Shi Y, Zhao Y, Liu H, Li, X, Bai, M. Bai, Push–pull" 1,8-naphthalic anhydride with multiple triphenylamine groups as electron donor. J. Mole. Stru.2014; 1056: 339- 346. https://doi.org/10.1016/j.molstruc.2013.10.004.

[21] Bojinov V, Panova I. synthesis of novel fluorophores- combination of hindered amine and UV absorber in the molecule of BENZO[de]ISOQUINOLINE-1,3-DIONE. J. Univ. Chem. Technol. Metallurgy. 2006; 41 : 277- 284.

[22] Banerjee S, Kitchen JA, Gunnlaugsson T, Kelly JM. Synthesis and photophysical evaluation of a pyridinium 4-amino-1,8-naphthalimide derivative that upon intercalation displays preference for AT-rich double-stranded DNA. J. M. Kelly, Org. Biomol. Chem. 2012; 10 : 3033- 3043. https://doi.org/10.1039/C2OB06898B.

[23] Orhan E. Synthesis of Novel Diarylethenes Bearing Naphthalimide Moiety and Photochromic Fluorescence Behaviors. JOTCSA. 2017; 4:501-516. https://doi.org/10.18596/jotcsa.296370.

[24] Ventura B, Bertocco A, Braga D, Catalano L, d'Agostino S, Grepioni F, Taddei P. Luminescence Properties of 1,8-Naphthalimide Derivatives in Solution, in Their Crystals, and in Co-crystals: Toward Room-Temperature Phosphorescence from Organic Materials. J. Phys. Chem. C. 2014; 118 : 18646- 18658.https://doi.org/10.1021/jp5049309.

[25] SOLTANI PH, KHOSRAVI A, GHARANJIG K, KHORASANI M, Khatibzadeh M, AFSHAR TF. Synthesis and Characterization of New Fluorescent Polymerizable Dyes Based on Naphthalimide. Iran. Polym. J. 2010; 19: 491- 500. http://journal.ippi.ac.ir.

[26] Saito G, Velluto D, Resmini, M . Synthesis of 1,8-naphthalimide-based probes with fluorescent switch triggered by flufenamic acid. R. Soc. open sci. 2018; 5 (6) : 1- 12. https://doi.org/10.1098/rsos.172137.

[27] Akinbulumo OA, Odejobi OJ, Odekanle EL. Thermodynamics and adsorption study of the corrosion inhibition of mild steel by Euphorbia

heterophylla L. extract in 1.5 M HCl. Results in Materials. 2020; 5 : 100074. https://doi.org/10.1016/j.rinma.2020.100074.

[28] Bhatt Y, Kumari P, Sunil D, Rao SA, Shetty P, Kagatikar S. The impact of naphthalimide derivative on the mitigation of mild steel corrosion in sulfamic acid medium: experimental and theoretical insights. Chemical Papers. 2021; 75: 3831-3845. https://doi.org/10.1007/s11696-021-01608-9.

[29] Yönten V, Sanyürek NK, Kivanç MR. A thermodynamic and kinetic approach to adsorption of methyl orange from aqueous solution using a low cost activated carbon prepared from Vitis vinifera L. Surfaces and Interfaces. 2020; 20 : 100529. https://doi.org/10.1016/j.surfin.2020.100529.

[30] Mir JM, Maurya RC, Vishwakarma PK. Corrosion resistance and thermal behavior of acetylacetonato-oxoperoxomolybdenum (VI) complex of maltol: experimental and DFT studies. KIJOMS. 2017; 3(4): 212-223. https://doi.org/10.1016/j.kijoms.2017.08.006.

[31] Ashraf M, Ramzan N, Khan RU, Durrani AK. Analysis of mixed cattle manure: Kinetics and thermodynamic comparison of pyrolysis and combustion processes. Case Stud. Therm. Eng. 2021;26:101078. https://doi.org/10.1016/j.csite.2021.101078.

[32] Iben Ayad A, Luart D, Ould Dris A, Guénin E. Kinetic analysis of 4-nitrophenol reduction by "water-soluble" palladium nanoparticles. Nanomaterials. 2020; 10(6) : 1169. https://doi.org/10.3390/nano10061169.

[33] Hemed SJ. A comparative study between the atomic absorption and spectrophotometric method in the assessment of the corrosion. JUK. 2011; 9(4) : 21-25. 395fdf59ce9ced78.

[34] Al-Rumaihi A, Parthasarathy P, Fernandez A, Al-Ansari T, Mackey HR, Rodriguez R, McKay G. Thermal degradation characteristics and kinetic study of camel manure pyrolysis. J. Environ. Chem. Eng. 2021; 9 (5) :106071. https://doi.org/10.1016/j.jece.2021.106071.

[35] Ali I, Tariq R, Naqvi SR, Khoja AH, Mehran MT, Naqvi M, Gao N. Kinetic and thermodynamic analyses of dried oily sludge pyrolysis. J. Energy Inst. 2021; 95 :30-40. https://doi.org/10.1016/j.joei.2020.12.002.

[36] Ayoola AA, Babalola R, Durodola BM, Alagbe EE, Agboola O, Adegbile EO. Corrosion inhibition of A36 mild steel in 0.5 M acid medium using waste citrus limonum peels. Results in Engineering. 2022; 15 :100490. https://doi.org/10.1016/j.rineng.2022.100490.

[37] Verma DK, Ebenso EE, Quraishi MA, Verma, C. Gravimetric, electrochemical surface and density functional theory study of acetohydroxamic and benzohydroxamic acids as corrosion inhibitors for copper in 1 M HCl. Results in Physics. 2019; 13: 102194. https://doi.org/10.1016/j.rinp.2019.102194.